Hindawi Publishing Corporation
Journal of Nanomaterials
Volume 2012, Article ID 902491, 6 pages
doi:10.1155/2012/902491

Research Article

Synthesis and Characterization of Electrospun Nanocomposite TiO_2 Nanofibers with Ag Nanoparticles for Photocatalysis Applications

Srujan Mishra and S. Phillip Ahrenkiel

Nanoscience and Nanoengineering Department, South Dakota School of Mines and Technology, Rapid City, SD 57701, USA

Correspondence should be addressed to Srujan Mishra, srujan.mishra@mines.sdsmt.edu

Received 18 October 2011; Accepted 9 November 2011

Academic Editor: Titipun Thongtem

Polycrystalline mixed-phase TiO_2 nanofibers embedded with 2.0% w/v Ag nanoparticles was prepared by the electrospinning technique. Calcination of dry Ag nanoparticles-titanium (IV) isopropoxide/PVP electrospun nanofiber mats in air at 510°C for 24 h yielded polycrystalline TiO_2/Ag nanofibers. The morphology and distribution of silver nanoparticles were observed by transmission electron microscopy (TEM), scanning TEM (STEM), and high-angle annular dark-field (HAADF) imaging. Mixed-phase anatase and rutile TiO_2 nanofibers were produced with Ag nanoparticles. High-resolution TEM lattice-fringe measurements showed good agreement with Ag (111), anatase (101), and rutile (110) phases. The photocatalytic activity of TiO_2/Ag nanofibers was compared to the photocatalytic activity of pure TiO_2 nanofibers by studying the photodegradation of methyl red dye under UV light irradiation, in a photoreactor. UV-visible absorbance spectra showed that the rate of decay of the dye in case of photodegradation by TiO_2/Ag nanofibers was 10.3 times higher than that by pure TiO_2 nanofibers. The retaining of the fiber morphology along with the increased surface area due to the addition of Ag nanoparticles can be believed to enhance the photocatalytic oxidation of methyl red dye.

1. Introduction

Electrospinning is a versatile jet-based method, which is used for producing nanofibers from many polymeric precursors. The dispersion of metal nanoparticles into polymer nanofibers is of great interest because of not only the novel properties of the nanocomposite materials but also continuously growing demand for further miniaturization of electronic components, optical detectors, chemical and biochemical sensors, and devices [1]. Fiber membranes have been shown to be very useful for heterogeneous catalysis and also as supports for catalytic metal nanoparticles and nanowires [2]. Compared to conventional film photocatalysts, nanofibers-based photocatalysts have greater surface-to-volume ratio, and its porous structure allows for higher surface active sites for effective catalysis. Titania is a wide band gap semiconductor material with many important applications including solar cell and photocatalysis. Titania has two common crystalline forms; rutile and anatase. Anatase titania, with an octahedral crystalline structure and a band gap of 3.2 eV, exhibits high activities for use in solar cell and photocatalysis [3]. Anatase titania can be excited under UV light and rutile under visible light. The production of mixed-phase anatase and rutile nanocrystalline fibers is beneficial. Incorporation of noble metal nanoparticles is a recent method to enhance the photocatalytic behavior of titania. Nanostructured noble metals are believed to be excellent heterogeneous catalysts [4–7]. The incorporation of Ag nanoparticles can increase the catalytic activity of TiO_2 nanocomposite fiber membranes, and the mechanism has been well explained in many research articles [8–10].

In the present study, we have established a successful method of incorporating Ag nanoparticles in TiO_2 nanofibers by electrospinning and calcination. The produced crystalline nanofibers were used as photocatalysts to study

the photodegradation of an acidic dye, methyl red, under UV light irradiation.

2. Experimental

2.1. Materials. Poly (vinyl pyrrolidone) (PVP, CAS# 9003-39-8, M_w = 1,300,000) and titanium (IV) isopropoxide (TiIP, CAS# 546-68-9, 99.995%, metals basis) were purchased from Alfa Aesar (Ward Hill, Massachusetts). Methyl red (powder), absolute ethanol, and acetic acid were purchased from Fisher Scientific (Pittsburgh, Pennsylvania). Ag nanopowder (99.99% pure, 15 nm in average size) was purchased from M K Nano (Missisauga, Ontario). All chemicals were used without any further purification.

2.2. Precursor Solution Preparation. Many different precursor solutions were selected for this research. The solutions varied in the concentrations of the different constituents. Extensive research has been done on the stability of PVP-based nanofiber systems [11, 12]. Also, PVP is an excellent capping reagent of various metal nanoparticles. Hence, PVP was chosen as the primary binding polymer. 10% w/v PVP solution was prepared by dissolving PVP powder in ethanol (EtOH) and stirring for 3 h at room temperature. A stock solution of 10 vol% Ag nanoparticles in EtOH was prepared for use in precursor preparation.

Two TiO_2 nanofiber-precursor solutions, with Ag nanoparticles, were prepared by mixing Ag-EtOH solution in a titania precursor solution containing PVP (0.6 g, 10% w/v), TiIP, and acetic acid (0.25 mL, 3 vol%) in EtOH, to prepare solutions with a final Ag NP concentrations of 2.0% and 0.68% w/v. The solutions were continuously stirred for 3 h until it got a greenish tinge. The precursor solution with 2.0% Ag was optimized and chosen for further analysis.

2.3. Electrospinning. A specially designed vertical electrospinning apparatus was used to conduct the experiments. It consisted of a high voltage power supply (Glassman High Voltage, Inc., High Bridge, NJ) capable of up to 30 kV DC output and a 10 mL standard syringe with a stainless steel needle having a 0.5 mm orifice. A setup was made to apply varying loads on the syringe plunger head to control the flow rate of the precursor solution. An electrically grounded brass plate was used to hold the aluminum foil, which served as the collector. During all electrospinning experiments a positive high voltage of 15 kV was applied and a distance of 5″ was maintained between the tip of the syringe needle and the aluminum collector. The sol-gel precursor was loaded in the 10 mL syringe and electrospinning was carried out with a solution flow rate of 1.0 mL/h. The electrospinning was carried out at room temperature under a fume hood for 3 h after which, the nonwoven mat of fibers was allowed to stand for 2 h at room temperature to dry off the solvent.

2.4. Annealing. Optimal conditions for pyrolysis were established to completely burn off the PVP while retaining good nanofiber morphology composed of crystalline TiO_2, predominately in the anatase phase. For annealing temperature greater than 650°C, the fibers completely crystallize as rutile, whereas complete pyrolysis of PVP does not occur below 450°C. Based upon extensive investigations, an optimal annealing temperature of 510°C was established. To perform annealing, the as-spun nanofibers were placed in a heating oven for drying at 60°C for 1 h. A portion of the dried material was then peeled off the aluminum foil and transferred to a ceramic boat for annealing in a Carbolite tube furnace at 510°C for 24 h, with a continuous flow of air. The annealed fibers were allowed to cool slowly to room temperature after the 24 h heating cycle.

2.5. Photoreactor Setup. To measure the photocatalytic activity of pure TiO_2 and TiO_2/Ag nanofibers, a simple photoreactor setup was made. Methyl red dye was prepared to 1.01 mM concentration in distilled water and filtered to remove undissolved particles. The photoreactor setup consisted of a glass beaker containing 100 mL of methyl red dye with 50 mg of photocatalyst material. This solution was continuously stirred under an ultraviolet lamp source, emitting at 365 nm, for UV irradiation. At certain time intervals 3 mL of the dye was withdrawn from the reactor and subjected to centrifugation to allow the solid catalyst material to settle down at the bottom. Absorbance intensities were measured for the dye samples at different time intervals, at a particular absorbance wavelength.

2.6. Characterization. Transmission electron microscopy (TEM) characterization was performed on a JEOL JEM 2100 high-resolution TEM operated at 200 kV, with a scanning TEM (STEM) system for dark-field and bright-field analysis, selected area diffraction analysis and equipped with an Oxford Inca energy-dispersive silicon-drift X-ray (EDX) spectrometer for compositional analysis. Image acquisition was performed with a Gatan Orius bottom mount, 14-bit, 11-megapixel CCD camera. X-ray diffraction (XRD) analysis was done using a powder X-ray diffractometer. Rotating-detector scan was done over a range of 2θ angles from 20° to 80°. Absorbance measurements on the methyl red dye during photocatalytic degradation were carried out by spectroscopic analysis using a Perkin Elmer Lambda 650 UV-visible spectrometer. The absorbance scans were run over the wavelength range of 350 to 700 nm. The spectra were obtained using UV WinLab software and were analyzed using Igor Pro 6.12 software.

3. Results and Discussion

TiO_2 has been proved to be an excellent photocatalyst material that can absorb ultraviolet radiation from sunlight or any illuminated light source (fluorescent lamps), to produce pairs of electrons and holes. This is referred to as the photo-excitation stage. The wavelength (λ) of light necessary for photo-excitation is given by $\lambda = hc/E$, where h is the Planck's constant, c is the velocity of light in vacuum, and E is the band gap energy (= 3.2 eV for anatase TiO_2). For TiO_2, it turns out that λ = 388 nm. The high band gap of anatase

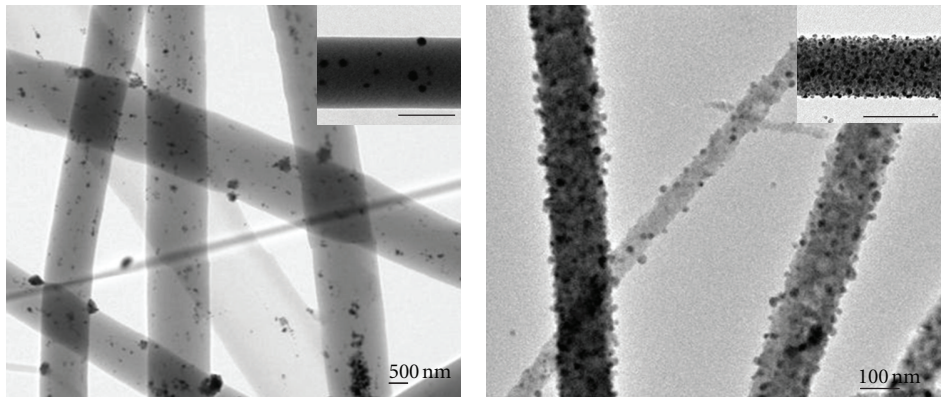

(a) (b)

Figure 1: STEM images of (a) amorphous TiIP/PVP/Ag nanofibers and (b) polycrystalline TiO_2/Ag nanofibers, both with 2% w/v Ag nanoparticles. Images in the inset are high-magnification TEM images of respective samples. The scale bars in the inset are 200 nm.

TiO_2 along with the photo-excitation wavelength in the near-UV range makes it an interesting photo-catalytic material.

3.1. Structural Characterization of TiO_2/Ag Nanofibers. PVP has been extensively used as a carrying polymer in fabricating various nanofibers. PVP is also soluble in many common solvents like water, isopropyl alcohol, ethanol, and many others. The low toxicity and suitable thermal properties of PVP make it a good carrying polymer. Ethanol has been reported to be a good candidate as a solvent in electrospinning of polymer nanofibers [11]. We selected titanium (IV) isopropoxide (TiIP) as the precursor for electrospinning TiO_2 nanofibers. TiIP could be directly added to EtOH and it formed a stable solution. In addition to PVP, acetic acid was also added to stabilize the solution and to control the hydrolysis reactions of the sol-gel precursor.

The average size of the Ag nanoparticles used to incorporate into the TiO_2 nanofibers was 15 nm. The *d*-spacing of the Ag (111) plane measured using fast Fourier transform (FFT) of a high-resolution TEM image was 0.23 nm, which is consistent with literature data [13]. Figure 1(a) shows a representative STEM image of the as-spun TiIP nanofibers embedded with Ag nanoparticles in 2.0% w/v with PVP as the binder. The STEM and the high-magnification TEM image in the inset show the presence of Ag nanoparticles inside the nanofibers. The Ag nanoparticles were uniformly distributed throughout the fiber length.

Figure 1(b) shows the nanocrystalline TiO_2/Ag nanofibers after calcination at 510°C for 24 h. Note that the fibers have a smaller diameter compared to the as-spun fibers. This is due to the complete pyrolysis of PVP. The calcined fibers were found to be completely crystalline. Powder X-ray diffraction (XRD) analysis of the crystalline TiO_2/Ag nanofibers, presented in Figure 2 shows the presence of anatase, rutile, and silver peaks. The peaks are labeled "A" for anatase, "R" for rutile, and "S" for silver. The diffraction peaks for anatase correspond to the crystal planes (101), (200), (211), (118), (220), and (215). Peaks corresponding to rutile crystal planes (110), (101), (111),

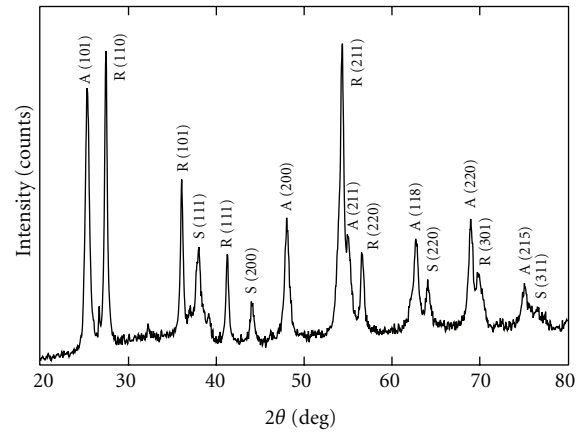

(A) Anatase TiO_2
(R) Rutile TiO_2
(S) Silver

Figure 2: XRD pattern of polycrystalline TiO_2/Ag nanofibers prepared by calcination of amorphous TiIP/PVP/Ag nanofibers at 510°C for 24 h. Anatase, rutile, and silver peaks are indicated by "A", "R" and "S" respectively.

(211), (220), and (301) could be found. The presence of peaks corresponding to silver crystal planes (111), (200), (220), and (311) is indicative of elemental Ag present in the nanofibers. This showed that the TiO_2 nanofibers did retain Ag nanoparticles in their elemental form. Quantitative analysis from the profile-fitted peaks of the XRD data showed that there was 48.9 vol% rutile, 45.8 vol% anatase, and about 2.1 vol% silver.

Figure 3(a) is a TEM image of a single TiO_2/Ag nanofiber. As it can be seen from the image, the TiO_2 nanofiber looks polycrystalline. There is evidence of small particles everywhere. Upon high-resolution TEM analysis, we found that those small particles were silver. The *d*-spacing measurements from the FFT image shows close match to the Ag (111) crystal plane (Figure 3(b)). High-resolution TEM

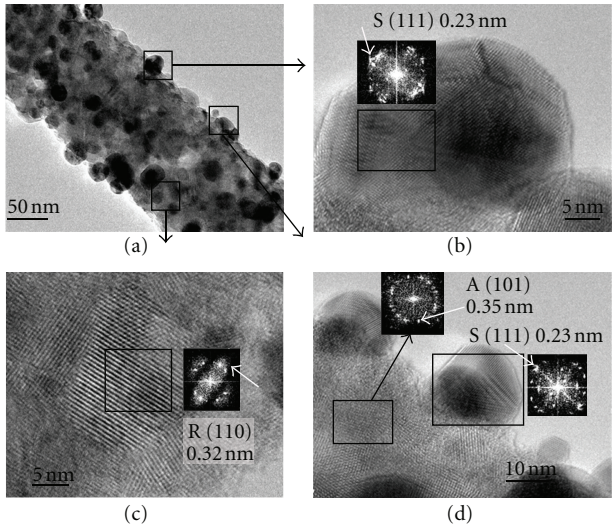

Figure 3: (a) TEM image of crystalline TiO_2/Ag nanofibers after calcination. (b, c, and d) High-resolution TEM images of corresponding highlighted regions in (a), showing lattice fringes corresponding to Ag (111), rutile (110), and anatase (101) planes. Insets show FFT patterns of highlighted regions in respective images, and the white arrows point at the corresponding lattice points.

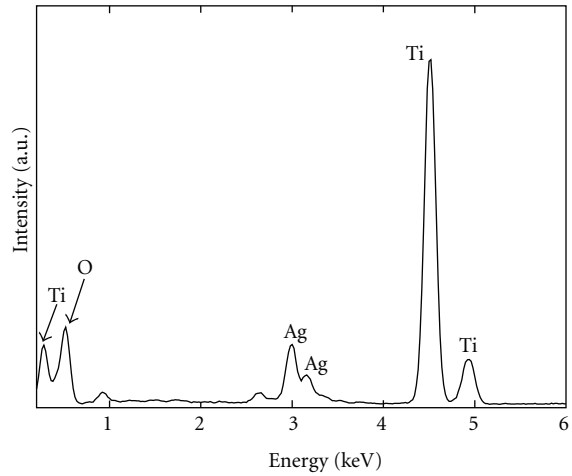

Figure 4: EDX spectrum from a representative area of the calcined TiO_2/Ag nanofibers showing presence of Ti, O, and Ag.

images taken from different parts of the TiO_2/Ag nanofibers showed presence of anatase and rutile titania. Figure 3(c) is a high-resolution TEM image showing the rutile grains in the nanofiber. The FFT image of the square area suggests that the *d*-spacing of 0.32 nm corresponds to the rutile (110) crystal planes. Figure 3(d) shows evidence of anatase (101) planes and Ag (111) planes. These results support our previous analysis that the produced TiO_2/Ag nanofibers had a mixed-phase anatase-rutile polycrystalline structure with Ag nanoparticles.

TEM-EDX analysis was done to confirm the presence of Ag nanoparticles. In Figure 4, the EDX spectrum obtained

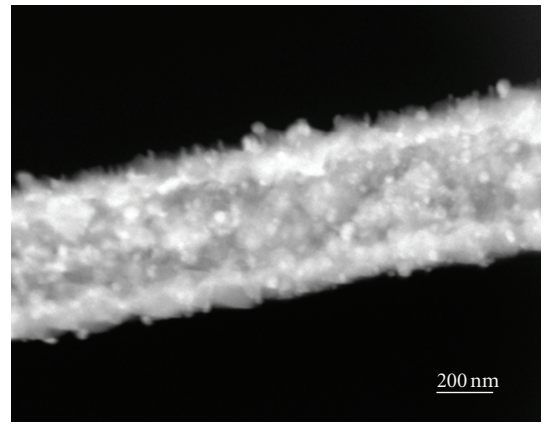

Figure 5: HAADF image taken using the STEM detector. Bright spots in the image represent the higher atomic number element (Ag) dotted along the nanofibers. Less bright areas represent TiO_2.

from a representative area of the nanofibers showed the presence of Ti, O, and Ag peaks. In order to study the distribution of Ag nanoparticles in the nanofibers, we chose to perform STEM-HAADF analysis. Figure 5 shows a HAADF image of a representative area of the nanofiber sample. In HAADF imaging, the larger atomic number (Z) elements appear brighter than the lower Z elements. This can help us distinguish between the crystalline Ag and titania phases. Bright white spots can be seen dotted all along the fibers. Due to its higher Z, the bright spots are identified as Ag nanoparticles, some of which clearly reside on the fiber surfaces. This confirms the presence of Ag as nanoparticles and not as any solid-solution alloy of silver and titania.

3.2. Photocatalytic Activity Study. To study the photocatalytic activity of the TiO_2/Ag nanofibers, methyl red dye was chosen. Methyl red dye has been widely used to measure catalytic activity of titania nanostructures [2, 14, 15] and is considered as a good model compound to evaluate the catalytic activity of Ag doped TiO_2 nanofibers and hence the choice. Upon exposure to UV light, we found that methyl red dye did not decay substantially during the course of the experiment.

We know that the concentration of a solution is in linear relationship with its absorbance (A) at a specific wavelength maximum (λ_{max}). From Beer-Lambert law, for a liquid solution,

$$A = -\log_{10} T = \varepsilon b C, \tag{1}$$

where T is the transmittance, ε is the molar absorptivity, b is the path length of the sample, and C is the concentration of the solution. The photocatalysis reaction was carried out to study the dye decay behavior of methyl red dye due to TiO_2/Ag nanofibers and was compared to the results with pure, crystalline, calcined TiO_2 nanofibers. In the photocatalysis experiment, 3 mL of dye sample was withdrawn from the reactor and centrifuged for about 20 min to allow for catalyst material to settle. Upon measuring the absorbance of the methyl red dye, it was found that the dye

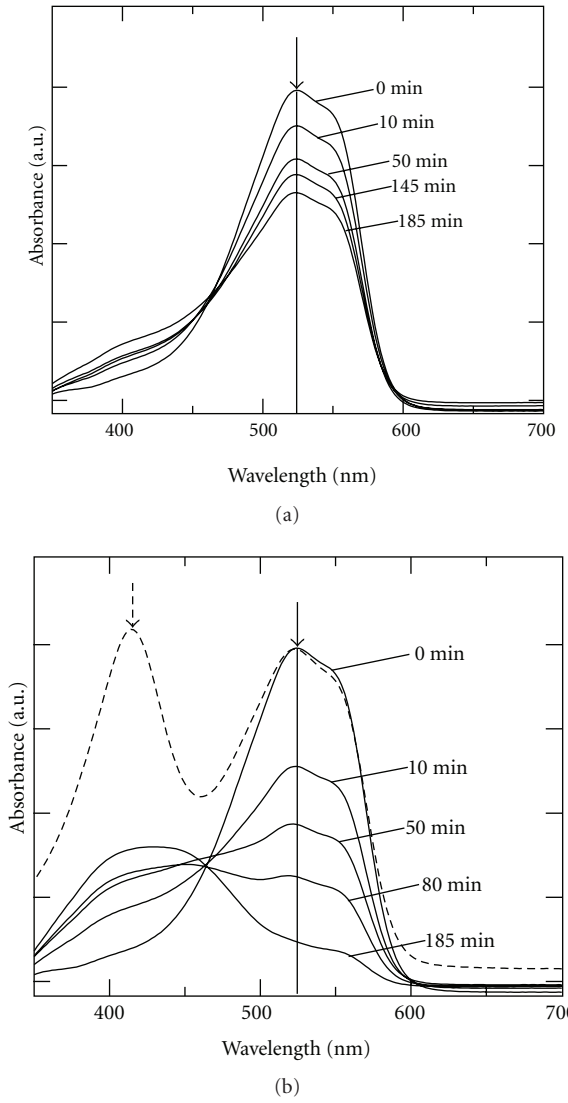

Figure 6: UV-visible spectra of methyl red dye taken at different time intervals during the photodegradation by: (a) pure TiO_2 nanofibers and (b) TiO_2/Ag nanofibers. Methyl red dye had the λ_{max} peak at 524 nm. The dashed curve in (b) represents the UV-visible spectrum of methyl red dye with Ag nanoparticles in solution. Solid arrow represents methyl red peak at 524 nm. The dashed arrow represents peak at 414 nm corresponding to Ag nanoparticles.

had maximum absorbance at $\lambda_{max} = 524$ nm. Figures 6(a) and 6(b) show the absorbance plots of the methyl red dye during photocatalysis by pure TiO_2 and TiO_2/Ag nanofiber catalysts, respectively. The absorbance spectra from the dye are collected at time intervals of 0, 10, 20, 30, 40, 50, 60, 70, 80, 90, 100, 125, 135, 145, 155, 165, 175, and 185 min. The dashed curve in the Figure 6(b) represents the absorbance curve for a solution containing methyl red dye and Ag nanoparticles at a certain concentration. This explains the appearance of a second peak at 414 nm, which corresponds to Ag nanoparticles. The second, much smaller peak appears with increasing Ag nanoparticle concentration. We attribute this to the release of free Ag nanoparticles

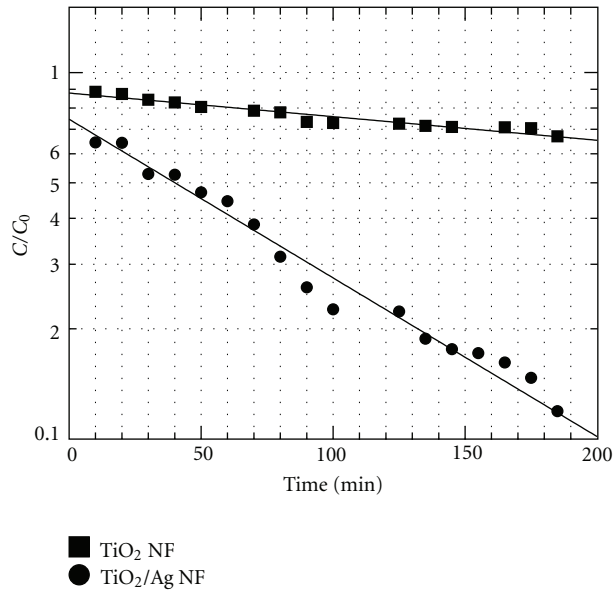

Figure 7: Effect of 185 min UV irradiation of TiO_2/Ag (circles) and TiO_2 (squares) nanofibers on methyl red dye. Plotted on a semilog scale, an exponential fit to the data points suggested a higher decay rate of the dye due to activity of TiO_2/Ag nanofiber catalysts.

into the solution. Absorbance of the methyl red dye after the 185 min photocatalysis experiment was compared to that of a solution containing Ag nanoparticles equivalent to the amount present in 50 mg nanofiber photocatalyst. From the ratio of the absorbance of the Ag nanoparticle soultion, to that of the dye containing free Ag nanoparticles, we estimate a gradual transfer to the dye of approximately 7% of the initial Ag nanoparticle content during the 185 min photoreaction, which we attribute to agitation due to stirring. Further experiments are planned to determine whether the loss from the solid of these weakly attached Ag nanoparticles has a significant effect on photocatalytic activity of the remaining nanofiber product.

The degree of photocatalytic degradation, η, can be calculated using the equation,

$$\eta = \frac{C}{C_0}, \tag{2}$$

where C_0 is the concentration of the dye at time $t = 0$, and C is the concentration of the dye at different time intervals. The concentration of the dye was then plotted against the irradiation time on a semilog graph for dye decay by pure TiO_2 and TiO_2/Ag nanofibers (Figure 7). Note that a rapid reduction in absorbance occurred upon contact of the dye solution with the solid nanofibers. Thus, the initial ($t = 0$) absorbance values were excluded from the fits. The remaining points were fit to an exponential decay function,

$$\frac{C(t)}{C_0} = r \cdot e^{-kt}, \tag{3}$$

where $C(t)$ is the concentration of the dye at time t, k is the rate of the reaction, and r is the relative concentration

Table 1: Decay rates (k) of the photodegradation of methyl red dye by TiO_2- and TiO_2/Ag-nanofiber photocatalysts.

Photocatalyst	Decay rate, k (min^{-1})
TiO_2 nanofibers	0.91×10^{-3}
TiO_2/Ag nanofibers	9.4×10^{-3}

of the exponential region, extrapolated to $t = 0$. The rates were corrected for a small dye decay rate of $0.57 \times 10^{-3}\,min^{-1}$ under UV illumination without any catalyst. Under UV irradiation, the dye showed a decay rate of $k = 0.91 \times 10^{-3}\,min^{-1}$ due to photodegradation in the presence of pure TiO_2 nanofibers, and a decay rate of $k = 9.4 \times 10^{-3}\,min^{-1}$ due to the photodegradation by TiO_2/Ag nanofibers (Table 1), with a ratio of 10.3. This represents a roughly tenfold increase in the photocatalytic decay rate of methyl red dye in the presence of TiO_2/Ag nanofibers compared to pure TiO_2 nanofibers. This result demonstrates that the presence of Ag has an enhanced effect on the catalytic property of TiO_2 nanofibers. The presence of Ag nanoparticles on the surface of the TiO_2 nanofibers can act as electron-trapping agents to dissociate photogenerated electron-hole pairs that can inhibit charge separation [16].

4. Conclusions

Nanocomposite mixed-phase polycrystalline TiO_2/Ag nanofibers were prepared by adding Ag nanoparticles to the TiIP precursor solution, followed by electrospinning and calcination at 510°C for 24 h. The uniform distribution of Ag nanoparticles in the electrospinning precursor results in the residence of Ag nanoparticles on the rough, porous surface of the TiO_2 nanofibers, resulting in a strong enhancement of photocatalytic activity, with respect to TiO_2 fibers synthesized without Ag, as measured by the photocatalytic oxidation of methyl red dye under UV illumination. This study demonstrates a simple route to functionalization of electrospun, titania nanofibers for enhanced photocatalytic activity, with possible applications in photovoltaics.

Acknowledgment

This work was supported by the US Department of Energy, Contract no. DE-FG02-08ER64624.

References

[1] Y. Wang, Y. Li, G. Sun et al., "Fabrication of Au/PVP nanofiber composites by electrospinning," *Journal of Applied Polymer Science*, vol. 105, no. 6, pp. 3618–3622, 2007.

[2] E. Formo, E. Lee, D. Campbell, and Y. Xia, "Functionalization of electrospun TiO_2 nanofibers with Pt nanoparticles and nanowires for catalytic applications," *Nano Letters*, vol. 8, no. 2, pp. 668–672, 2008.

[3] M. R. Hoffmann, S. T. Martin, W. Choi, and D. W. Bahnemann, "Environmental applications of semiconductor photocatalysis," *Chemical Reviews*, vol. 95, no. 1, pp. 69–96, 1995.

[4] R. Ma, T. Sasaki, and Y. Bando, "Layer-by-layer assembled multilayer films of titanate nanotubes, Ag- or Au-loaded nanotubes, and nanotubes/nanosheets with polycations," *Journal of the American Chemical Society*, vol. 126, no. 33, pp. 10382–10388, 2004.

[5] J. Huang, T. Kunitake, and S. Y. Onoue, "A facile route to a highly stabilized hierarchical hybrid of titania nanotube and gold nanoparticle," *Chemical Communications*, vol. 10, no. 8, pp. 1008–1009, 2004.

[6] H. Tada, K. Teranishi, Y. I. Inubushi, and S. Ito, "Ag nanocluster loading effect on TiO_2 photocatalytic reduction of bis(2-dipyridyl)disulfide to 2-mercaptopyridine by H_2O," *Langmuir*, vol. 16, no. 7, pp. 3304–3309, 2000.

[7] M. Jin, X. Zhang, A. V. Emeline et al., "Fibrous TiO_2-SiO_2 nanocomposite photocatalyst," *Chemical Communications*, no. 43, pp. 4483–4485, 2006.

[8] H. M. Sung-Suh, J. R. Choi, H. J. Hah, S. M. Koo, and Y. C. Bae, "Comparison of Ag deposition effects on the photocatalytic activity of nanoparticulate TiO_2 under visible and UV light irradiation," *Journal of Photochemistry and Photobiology A*, vol. 163, no. 1-2, pp. 37–44, 2004.

[9] N. Sobana, M. Muruganadham, and M. Swaminathan, "Nano-Ag particles doped TiO_2 for efficient photodegradation of Direct azo dyes," *Journal of Molecular Catalysis A*, vol. 258, no. 1-2, pp. 124–132, 2006.

[10] M. Mrowetz, A. Villa, L. Prati, and E. Selli, "Effect of Au nanoparticles on TiO_2 in the photocatalytic degradation of an azo dye," *Gold Bulletin*, vol. 40, no. 2, pp. 154–160, 2007.

[11] D. Li and Y. Xia, "Fabrication of titania nanofibers by electrospinning," *Nano Letters*, vol. 3, no. 4, pp. 555–560, 2003.

[12] R. Chandrasekar, L. Zhang, J. Y. Howe, N. E. Hedin, Y. Zhang, and H. Fong, "Fabrication and characterization of electrospun titania nanofibers," *Journal of Materials Science*, vol. 44, no. 5, pp. 1198–1205, 2009.

[13] K. Yoshida, M. Makihara, N. Tanaka et al., "Specific surface area and three-dimensional nanostructure measurements of porous titania photocatalysts by electron tomography and their relation to photocatalytic activity," *Microscopy and Microanalysis*, vol. 17, pp. 264–273, 2011.

[14] M. A. Kanjwal, N. A. M. Barakat, F. A. Sheikh, W. I. Baek, M. S. Khil, and H. Y. Kim, "Effects of silver content and morphology on the catalytic activity of silver-grafted titanium oxide nanostructure," *Fibers and Polymers*, vol. 11, no. 5, pp. 700–709, 2010.

[15] M. A. Kanjwal, N. A. M. Barakat, F. A. Sheikh, M. S. Khil, and H. Y. Kim, "Functionalization of electrospun titanium oxide nanofibers with silver nanoparticles: strongly effective photocatalyst," *International Journal of Applied Ceramic Technology*, vol. 7, no. 1, pp. E54–E63, 2010.

[16] A. L. Linsebigler, G. Lu, and J. T. Yates Jr., "Photocatalysis on TiO_2 surfaces: principles, mechanisms, and selected results," *Chemical Reviews*, vol. 95, no. 3, pp. 735–758, 1995.